Inorganic Chemistry

Article

pubs.acs.org/IC

Intramolecular C−H Oxidative Addition to Iridium(I) in Complexes Containing a *N,N′*-Diphosphanosilanediamine Ligand

Vincenzo Passarelli,*[,†] Jesús J. Pérez-Torrente,[‡] and Luis A. Oro[‡]

[†]Centro Universitario de la Defensa, Ctra. Huesca s/n, ES−50090 Zaragoza, Spain

[‡]Departamento de Química Inorgánica, Instituto de Síntesis Química y Catálisis Homogénea-ISQCH, Universidad de Zaragoza-CSIC, Facultad de Ciencias, C/Pedro Cerbuna, 12, ES−50009 Zaragoza, Spain

Supporting Information

ABSTRACT: The iridium(I) complexes of formula Ir(cod)(SiNP)$^+$ (**1**$^+$) and IrCl(cod)(SiNP) (**2**) are easily obtained from the reaction of $SiMe_2\{N(4\text{-}C_6H_4CH_3)PPh_2\}_2$ (SiNP) with $[Ir(cod)(CH_3CN)_2]^+$ or $[IrCl(cod)]_2$, respectively. The carbonylation of [**1**][PF_6] affords the cationic pentacoordinated complex $[Ir(CO)(cod)(SiNP)]^+$ (**3**$^+$), while the treatment **2** with CO gives the cation **3**$^+$ as an intermediate, finally affording an equilibrium mixture of IrCl(CO)(SiNP) (**4**) and the hydride derivative of formula IrHCl(CO)(SiNP−H) (**5**) resulting from the intramolecular oxidative addition of the C−H bond of the $SiCH_3$ moiety to the iridium(I) center. Furthermore, the prolonged exposure of [**3**]Cl or **2** to CO resulted in the formation of the iridium(I) pentacoordinated complex Ir(SiNP−H)$(CO)_2$ (**6**). The unprecedented κ^3C,P,P' coordination mode of the [SiNP−H] ligand observed in **5** and **6** has been fully characterized in solution by NMR spectroscopy. In addition, the single-crystal X-ray structure of **6** is reported.

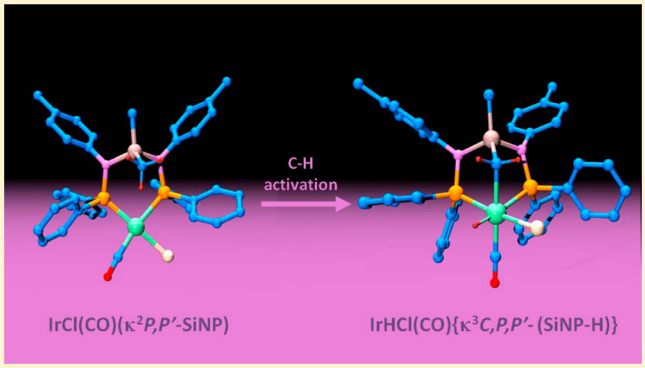

INTRODUCTION

The design of phosphano ligands containing P−N bonds has attracted a lot of interest, due to the easy functionalization and/or modification of the ligand backbone and to the consequent great versatility of these ligands both in coordination chemistry and in the study of stoichiometric and catalytic reactions.[1] Relevant to this paper, Scheme 1 shows selected diphosphano ligands containing the P−N functionality and different backbones and/or linkers. Interestingly, the coordination ability of $SiMe_2[(C_5H_4N\text{-}2)NPPh_2]_2$ (SiN^{py}P)[2] toward several transition metals has been described, and we have reported the synthesis of $SiMe_2\{N(4\text{-}C_6H_4CH_3)NPPh_2\}_2$ (SiNP)[3] and its reactivity toward rhodium. Despite the differences in the electronic and steric features of both SiN^{py}P and SiNP with respect to aliphatic diphosphanes like 1,2-bis(diphenylphosphano)ethane and 1,3-bis(diphenylphoshano)propane, both ligands always exhibit the expected κ^2P,P' coordination to the metal center (Scheme 1).

Scheme 1

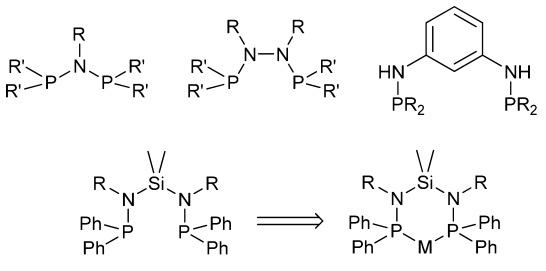

As far as SiNP in combination with rhodium is concerned, Scheme 2 shows selected examples of complexes featuring the κ^2P,P' coordination mode of SiNP.[3]

On this background, herein we describe the preparation and characterization of novel iridium(I) complexes with SiNP and the study of their reactivity. On one hand, it has been confirmed the predictable ability of SiNP to act as a bidentate κ^2P,P' ligand, and, on the other, it has been observed the unprecedented easy intramolecular oxidative addition of the $SiCH_2$−H bond to the iridium(I) center with the consequent formation of the [SiNP−H] ligand featuring a κ^3C,P,P' coordination mode.

RESULTS AND DISCUSSION

Synthesis of Iridium(I) Complexes. The iridium(I) complexes $[Ir(cod)(SiNP)]^+$ (**1**$^+$) and IrCl(cod)(SiNP) (**2**) (Scheme 3, cod = 1,5-cyclooctadiene) have been obtained by reaction of SiNP with $[Ir(cod)(CH_3CN)_2][PF_6]$ or $[IrCl(cod)]_2$, respectively (Scheme 3).[4]

In agreement with a square planar geometry at the metal center of $[Ir(cod)(SiNP)]^+$ (**1**$^+$), the $^{31}P\{^1H\}$ NMR spectrum

Received: September 26, 2013
Published: January 7, 2014

   dx.doi.org/10.1021/ic4024458 | Inorg. Chem. 2014, 53, 972−980

Scheme 2

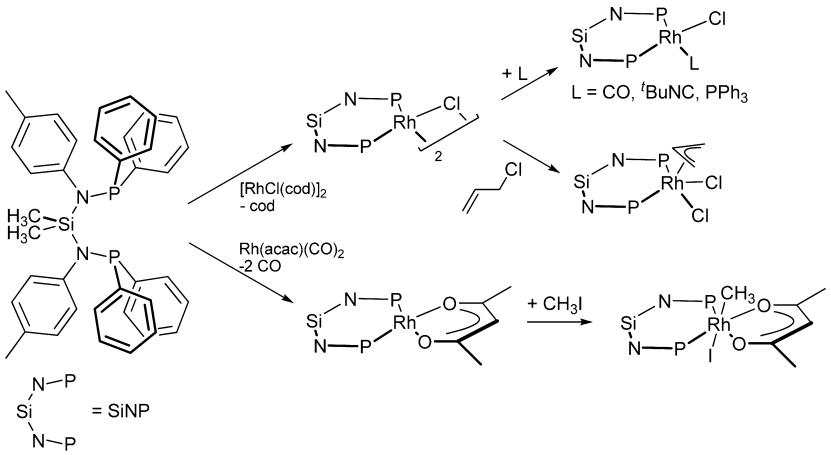

Scheme 3

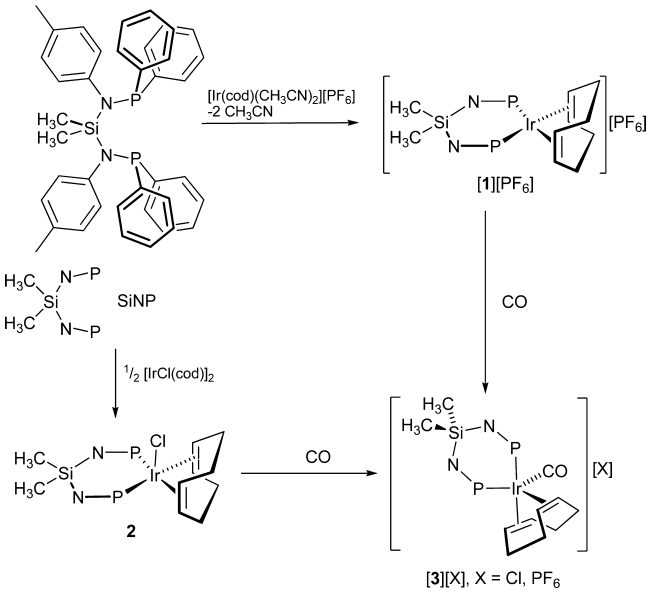

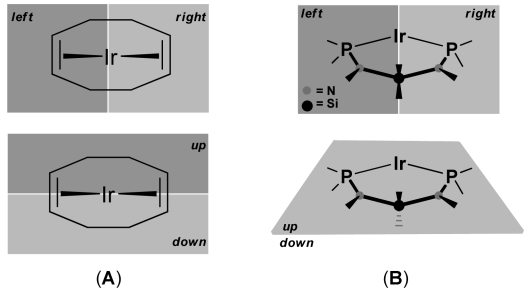

Figure 1. Definition of the left and right and the up and down semispaces at the coordinated cod (A) and the coordinated SiNP (B) ligands.

of $\mathbf{1}^+$ shows one singlet at 53.5 ppm for the SiNP ligand, and both equivalent tolyl groups and equivalent olefinic protons are observed (^{1}H, ^{13}C). Additionally, the ^{1}H and ^{13}C{^{1}H} NMR spectra show equivalent $SiCH_3$ moieties both at room temperature and at 183 K. On this basis, both the left and right and the up and down semispaces at the cod and the SiNP ligands (Figure 1) should be equivalent or eventually averaged by a fluxional process.

In agreement with the above-mentioned proposal, the optimized structures $\mathbf{1a}^+$ and $\mathbf{1b}^+$ of the cation $[Ir(cod)(SiNP)]^+$ ($\mathbf{1}^+$) (see DFT Geometry Optimization for details) show a slightly distorted square planar arrangement at the metal center with either a boat or a chair conformation of the SiN_2P_2Ir ring, respectively (Figure 2). The free energy difference between the two structures is 9.4 kJ mol^{-1}, the boat conformation being more stable than the chair conformation. Thus, the equivalence both of the olefinic cod protons and of the $SiCH_3$ methyls in $\mathbf{1}^+$ should be reasonably the consequence of the fast reversible interconversion $\mathbf{1a}^+ \leftrightarrows \mathbf{1b}^+$.

For the pentacoordinated iridium compound IrCl(cod)(SiNP) (**2**), an apparent symmetric environment at the metal center has been observed at room temperature. Indeed, similar to $\mathbf{1}^+$, one singlet at 49.4 ppm is observed in its ^{31}P{^{1}H} NMR spectrum, and the ^{1}H NMR spectrum indicates equivalent olefinic protons of the cod ligand and equivalent tolyl groups (see Experimental Section). Further, at room temperature, **2** shows a sharp ^{1}H singlet at 0.39 ppm for the $SiCH_3$ protons, and, even at 183 K, the ^{1}H and ^{31}P{^{1}H} NMR spectra are similar to those at room temperature, the only difference being slightly broader signals. Thus, the up and down and the left and right semispaces (Figure 1) both at the SiNP and at the cod ligands should be equivalent or averaged by a fluxional process. Starting from the ideal pentacoordinated configurations for IrCl(cod)(SiNP) shown in Figure 3, optimized structures of **2** were calculated by means of standard computational methods (see DFT Geometry Optimization for details), and the minimum free energy structure was found to be that derived from the SPY-5-13 configuration,[5] that is, a square pyramid containing the chlorido ligand at the apical position (Figure 4). Interestingly, this arrangement was previously observed in the solid-state structure of IrCl(cod)(dppb)[6] and IrCl(cod)(dppp).[7]

The optimized SPY-5-13 structure of **2**[8] features nonequivalent up and down semispaces both at the SiNP and at the cod ligands, but, as mentioned before, equivalent up and down semispaces (both at cod and at SiNP) were observed for **2** even at 183 K; thus a fluxional process exchanging the above-mentioned semispaces should be operative. In this relationship, it is noteworthy that the other optimized structures of **2**, that is, those derived from the SPY-5-32, SPY-5-23, TBPY-5-23, TBPY-5-12, and TBPY-5-13 configurations, Figure 3, were

dx.doi.org/10.1021/ic4024458 | Inorg. Chem. 2014, 53, 972−980

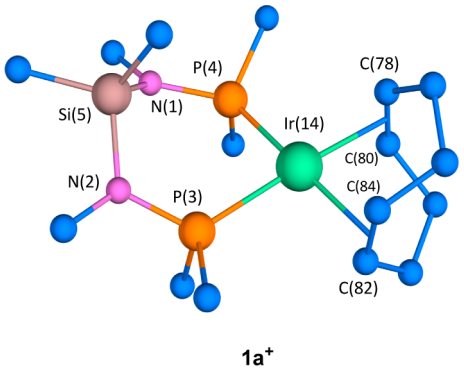

$1a^+$

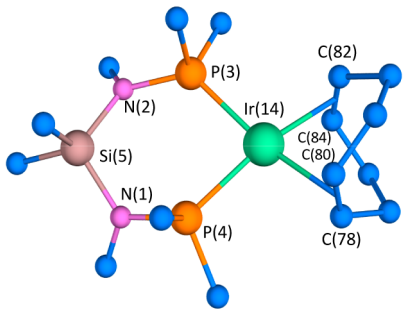

$1b^+$

Figure 2. Optimized structures of $[Ir(cod)(SiNP)]^+$ ($\mathbf{1}^+$) featuring a boat ($\mathbf{1a}^+$) and a chair ($\mathbf{1b}^+$) conformation at the SiN_2P_2Ir six-membered ring. Hydrogen atoms are omitted, and only *ipso* carbon atoms of the aromatic rings are shown for clarity (see the Supporting Information for atomic coordinates). Selected bond distances of the boat (normal type) and the chair (italics type) conformers (Å) are in order: Ir(14)−C(78), 2.248, *2.343*; Ir(14)−C(80) 2.236, *2.226*; Ir(14)−C(82) 2.235, *2.285*; Ir(14)−C(84) 2.279, *2.225*; Ir(14)−P(3) 2.413, *2.379*; Ir(14)−P(4), 2.380, *2.356*; C(78)−C(80) 1.405, *1.394*; C(82)−C(84) 1.398, *1.403*.

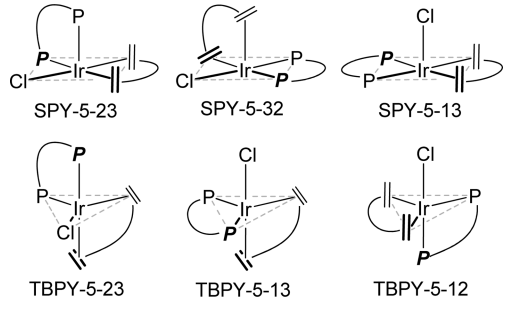

Figure 3. Pentacoordinated ideal configurations for IrCl(cod)(SiNP) (**2**).

found to be significantly less stable than the SPY-5-13 conformation with relative free energies higher than 65 kJ mol^{-1}. Thus, the up-down exchange via the reversible interconversion between different pentacoordinated structures can be ruled out. Furthermore, the gas-phase ΔG^0 values for the formation of a square planar complex via the dissociation from the metal either of the chlorido ligand (ΔG^0 = 459 kJ mol^{-1}) or of one double bond of the cod ligand (ΔG^0 = 122 kJ mol^{-1}) clearly indicate that none of the above-mentioned dissociation equilibria can be proposed to justify the observed exchange. On the other hand, the small free energy difference (+8.0 kJ mol^{-1}) between the optimized tetracoordinate square complex (SP-4-3) shown in Figure 4 and the SPY-5-13 structure and the affordable activation barrier calculated for the equilibrium SPY-5-13 ⇆ SP-4-3 ($\Delta H^{\ddagger}$ = 68.8 kJ mol^{-1}; $\Delta S^{\ddagger}$ = 15.4 J mol^{-1} K^{-1}) suggest that the reversible dissociation of one phosphorus atom from the metal center should be the process averaging the semispaces both at the cod and at the SiNP ligands.

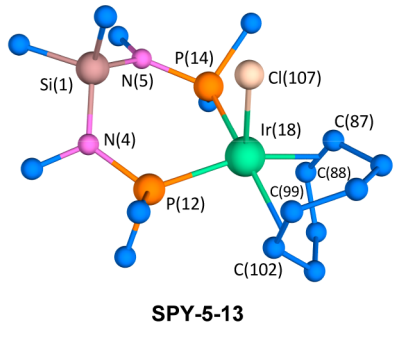

SPY-5-13

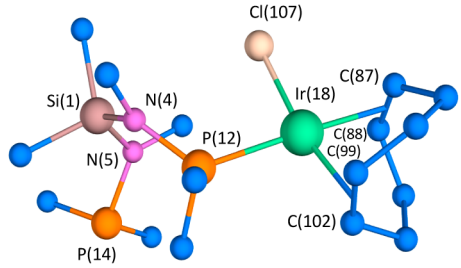

SP-4-3

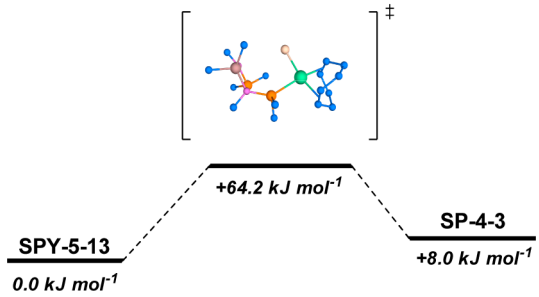

Figure 4. Optimized SPY-5-13 and SP-4-3 structures of **2** and the reaction profile for the equilibrium SP-5-13 ⇆ SP-4-3. Hydrogen atoms are omitted, and only *ipso* carbon atoms of the aromatic rings are shown for clarity (see the Supporting Information for atomic coordinates). Selected bond distances of **2** with the SPY-5-13 (normal type) and SP-4-3 (italics type) configurations (Å) are in order: Ir(18)−P(12), 2.393, *2.371*; Ir(18)−P(14), 2.407, *n.d.*; Ir(18)−C(87), 2.164, *2.234*; Ir(18)−C(88), 2.185, *2.188*; Ir(18)−C(99), 2.181, *2.166*; Ir(18)−C(102). 2.225, *2.132*; Ir(18)−Cl(107), 2.567, *2.382*; C(87)−C(88), 1.435, *1.402*; C(99)−C(102), 1.420, *1.428*.

CO-Promoted C−H Activation. The irreversible carbonylation of $[Ir(cod)(SiNP)]^+$ ($\mathbf{1}^+$) and IrCl(cod)(SiNP) (**2**) is fast and complete under mild conditions (1 atm of CO, room temperature, approx. 10 min) resulting in the formation of the pentacoordinated cation of formula $Ir(CO)(cod)(SiNP)^+$ $(\mathbf{3}^+)$[4] isolated as both [**3**]Cl and [**3**][PF_6], depending on the starting complex used in the synthesis (Scheme 3).

The IR spectrum of $\mathbf{3}^+$ (CH_2Cl_2 solutions) shows a strong ν_{CO} absorption at 1994 cm^{-1} in agreement with the presence of the coordinated CO ligand. At room temperature, the ^1H NMR

dx.doi.org/10.1021/ic4024458 | *Inorg. Chem.* 2014, 53, 972−980

spectrum of 3^+ shows nonequivalent $SiCH_3$ groups, thus indicating that nonequivalent up and down semispaces at SiNP exist (Figure 1). Further, equivalent phosphorus nuclei (^{31}P) and tolyl groups (^1H and ^{13}C) are observed at room temperature, while at 183 K the $^{31}P\{^1H\}$ NMR spectrum of 3^+ shows two signals (δ_P = 41.2, 37.3 ppm, see Supporting Information Figure E1) and accordingly two methyl ^1H resonances at 2.20 and 2.04 ppm for the tolyl moieties, as well. Thus, besides the up and down nonequivalence at the SiNP ligand observed at room temperature, also nonequivalent left and right semispaces should exist, and therefore a fluxional process should exchange them at room temperature (vide infra).

As far as the cod ligand is concerned, at room temperature its olefinic protons are totally equivalent, only one ^1H resonance being observed at 3.86 ppm. Nevertheless, at 183 K, the ^1H NMR spectrum of 3^+ shows four olefinic resonances (δ_H = 4.25, 3.20, 1.80, and 1.30 ppm; see Supporting Information Figure E3 for the assignment), indicating that both the up and down and the left and right semispaces at the cod ligand of 3^+ are nonequivalent at that temperature, and that the observed equivalence at room temperature results from a fluxional process averaging the above-mentioned semispaces. The ideal configurations matching the NMR spectroscopic data are SPY-5-12, SPY-5-23, and TBPY-5-12 (Figure 5). All of them were optimized by standard computational methods (see DFT Geometry Optimization for details), and the minimum free energy structure was found to be the TBPY-5-12 configuration shown in Figure 5,[9] the others featuring relative free energies higher than 70 kJ mol^{-1} with respect to TBPY-5-12. Noteworthy, similar to 1^+ and **2**, in the TBPY-5-12 structure,

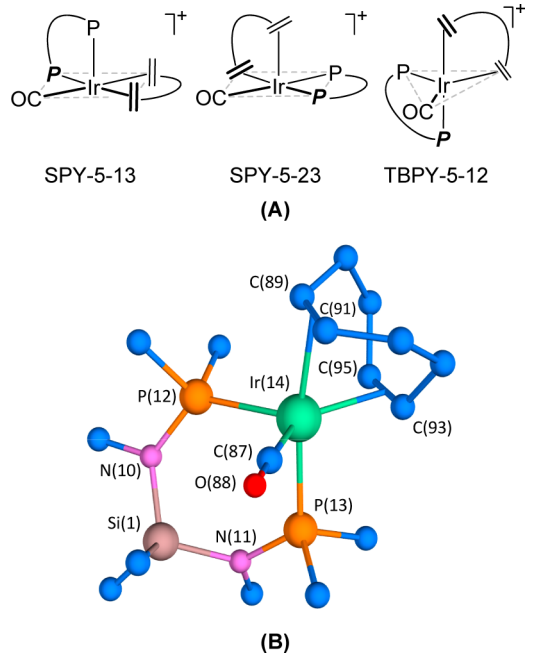

Figure 5. (A) Selected ideal configurations for $[Ir(CO)(cod)(SiNP)]^+$ (3^+). (B) Optimized TBPY-5-12 structure of 3^+. Hydrogen atoms are omitted, and only *ipso* carbon atoms of the aromatic rings are shown for clarity (see the Supporting Information for atomic coordinates). Selected bond distances (Å) are in order: Ir(14)–C(87), 1.922; Ir(14)–C(89), 2.361; Ir(14)–C(91), 2.345; Ir(14)–C(93), 2.177; Ir(14)–C(95), 2.196; Ir(14)–P(12), 2.518; Ir(14)–P(13), 2.428; C(87)–C(88), 1.155.

the boat conformation of the SiN_2P_2Ir ring was found to be more stable than the chair conformation (+16.6 kJ mol^{-1}).

As far as the possible fluxional processes affecting both the cod and the SiNP ligands are concerned, the nature of the ^1H NMR spectra (see Supporting Information Figure E3) prevented both the ^1H line shape analysis and the quantitative analysis of ^1H–^1H EXSY spectra at different temperatures. Nevertheless, the line shape analysis of the $^{31}P\{^1H\}$ resonances was easily carried out in the range 183–223 K affording the kinetic constants for the exchange of the left and right semispaces at the SiNP ligand. The activation parameters obtained from the Eyring plot ($\Delta H^{\ddagger}$ = 50.1 ± 0.5 kJ mol^{-1}; $\Delta S^{\ddagger}$ = 44.3 ± 2.6 J mol^{-1} K^{-1}; see Supporting Information Table E1 and Figure E2) and the fact that the exchange of the methyls of the $Si(CH_3)_2$ moiety is not observed reasonably indicate that the mechanism for the left–right exchange at the SiNP ligand is nondissociative. In this respect, it is worth mentioning that besides the TBPY-5-12 configuration, the TBPY-5-23 and the SPY-5-32 structures shown in Figure 6A

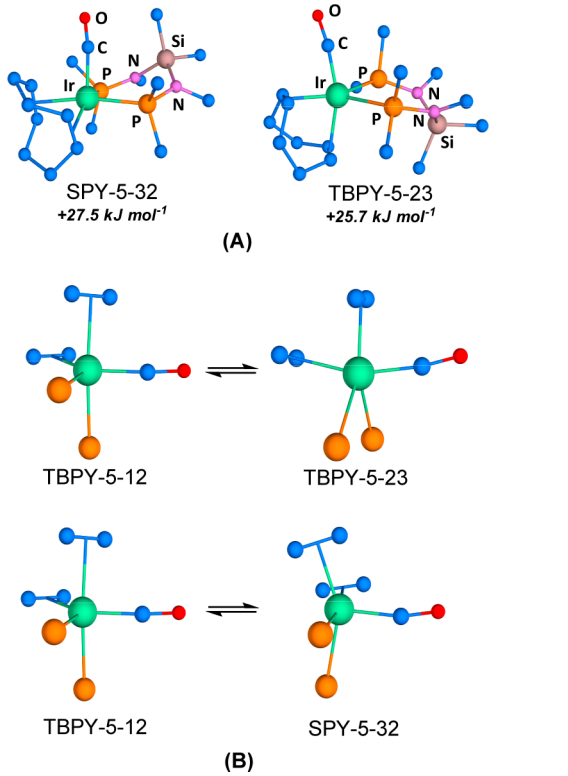

Figure 6. (A) Optimized SPY-5-32 and TBPY-5-23 structures of $[Ir(CO)(cod)(SiNP)]^+$ (3^+) with the relative free energies given with respect to TBPY-5-12. (B) Representation of the TBPY-5-12 ⇆ SPY-5-32 and TBPY-5-12 ⇆ TBPY-5-23 equilibria emphasizing the changes in the coordination sphere of the metal center.

were found to be local minima in the potential free energy surface, being located at +25.7 and +27.5 kJ mol^{-1}, respectively, with respect to the TBPY-5-12 structure. Thus, the equilibria TBPY-5-12 ⇆ SPY-5-32 and/or TBPY-5-12 ⇆ TBPY-5-23 (Figure 6B) should be operative in solution and could be responsible for the left–right exchange at the SiNP ligand.

Additionally, it is worth mentioning that these equilibria exchange the up and down (TBPY-5-12 ⇆ TBPY-5-23) and the left and right (TBPY-5-12 ⇆ SPY-5-32) semispaces at the cod ligand as well; thus reasonably they account also for the

dx.doi.org/10.1021/ic4024458 | *Inorg. Chem.* 2014, 53, 972–980

dependence on the temperature of the ^{1}H pattern of the cod ligand.

Dichloromethane solutions of [**3**]Cl are thermally unstable,[10] and the complete conversion of [**3**]Cl is observed in approximately 6 h at room temperature affording a mixture of IrCl(CO)(SiNP) (**4**)[4] and IrHCl(CO)(SiNP−H) (**5**)[4] with a molar ratio of 4:1, regardless of the concentration of [**3**]Cl. The ^{1}H and ^{31}P{^{1}H} NMR measurements indicate that at the beginning of the transformation of [**3**]Cl, the cod ligand is released and **4** is cleanly formed, no intermediate being detected even at 253 K. In addition, after approximately 15 min from the formation of **4**, measurable quantities of **5** are observed in the ^{1}H and ^{31}P{^{1}H} NMR spectra as the consequence of the activation of one C−H bond of the $SiCH_3$ group (Scheme 4).

Scheme 4. CO-Promoted C−H Activation in 3^+ (298 K)

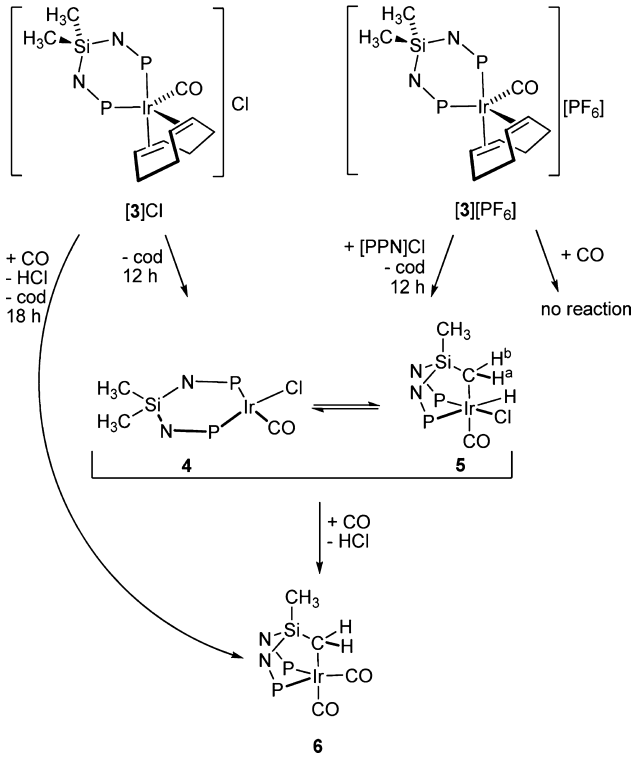

Interestingly, the CH_2Cl_2 solutions of [**3**][PF_6] are thermally stable, and the addition of equimolar amounts of [PPN]Cl resulted in the formation of the mixture **4**+**5** (4:1 molar ratio), as well. When the reaction was carried out varying the molar ratio $Cl^-/3^+$ (from 0.5 to 2), the same products, that is, **4** and **5**, and the same molar ratio between them, that is, 4:1, were observed.

The IR spectrum of a CH_2Cl_2 solution of the mixture **4**+**5** shows absorptions at 2007 (**4**) and 2026 cm^{-1} (**5**), indicating the presence of two species each containing coordinated carbon monoxide. The NMR spectrum of **4** suggests a square planar coordination of the metal center. Indeed, two nonequivalent phosphorus atoms are observed with the expected coupling constants for a cis arrangement ($^2J_{PP}$ = 30.5 Hz), and a ^{13}C{^{1}H} doublet-of-doublets is observed at 181.3 ppm ($^2J_{PC}$ = 124.3, 11.1 Hz), confirming that the CO ligand occupies the trans position with respect to one phosphorus and a cis one with respect to the other one. In agreement with the proposed arrangement of the donor atoms at the metal center of **4**, the tolyl groups are not equivalent (see Experimental Section). As a confirmation, the optimized structure of **4** features a square planar arrangement of the donor atoms at the metal center, and, similar to $\mathbf{1}^+$, **2**, and $\mathbf{3}^+$, the boat conformation of the SiN_2P_2Ir ring is calculated to be slightly more stable (6.4 kJ mol^{-1}) than the chair one (Figure 7). In this connection, the interconversion between the two conformers should be responsible for the observed equivalence between the $SiCH_3$ methyls.

When dealing with **5**, the spectroscopic data clearly indicate the presence of a hydride moiety and of the [SiNP−H] ligand featuring a κ^3C,P,P' coordination mode, both resulting from the intramolecular $SiCH_2$−H oxidative addition to the iridium(I) center of **4**. The ^{31}P{^{1}H} and ^{13}C{^{1}H} NMR spectra (see Supporting Information Figures E4 and E5) point unambiguously at the presence of two mutually cis phosphorus nuclei (δ_P = 48.1, 43.0 ppm, $^2J_{PP}$ = 9.0 Hz) with the carbon of the CO ligand cis to both of them (^{13}C{^{1}H} triplet at 172.48 ppm, $^2J_{PC}$ = 4.5 Hz). On the other hand, the coupling constants $^2J_{HP}$ of the hydride ligand (δ_H = −9.11 ppm) indicate that it occupies a cis position to one phosphorus ($^2J_{HP}$ = 18.0 Hz) and the trans one to the other ($^2J_{HP}$ = 177.9 Hz) (see Supporting Information Figure E6). Finally, the methylene carbon atom of the activated $SiCH_3$ group occupies a cis position with respect to both phosphorus atoms, and the coordination sphere of iridium should be completed by one chlorido ligand. In agreement with the proposed structure, nonequivalent tolyl groups (see Experimental Section) and nonequivalent methylenic hydrogen atoms are observed (δ_H = 0.79, H^a; 1.40 ppm, H^b). Further, the ^{1}H resonances for H^a and H^b show a pattern clearly indicating that H^b should feature a smaller dihedral angle with respect to the hydride moiety than H^a (Scheme 4, see Supporting Information Figure E6). Indeed, the scalar coupling constant of H^b with the hydride is 3.0 Hz, while no scalar coupling was observed between H^a and the hydrogen of the Ir−H moiety (see Supporting Information Figure E6). Because the Karplus curve for a H−X−Y−H system generally features a local maximum at the dihedral angle H−X−Y−H of 0° and a local minimum near 90°, the dihedral angle H^a−C−Ir−H should be close to 90°.[11]

As a confirmation, the proposed structure of **5** was optimized by standard computational methods (see DFT Geometry Optimization for details) and was found to feature a distorted octahedral arrangement of the donor atoms at the metal center with H^x−C−Ir−H dihedral angles of 100° (x = a) and 16° (x = b) in agreement with the above-mentioned $^3J_{HH}$ coupling constants (Figure 7). Additionally, it is worth mentioning that the calculated ν_{CO} wave numbers (**4**, 2017; **5**, 2029 cm^{-1}) are found close to the experimental ones (**4**, 2007; **5**, 2026 cm^{-1}).

Finally, the transition state structure for the transformation **4** ⇆ **5** was calculated[12] showing that the boat conformer of **4** allows the C−H bond to approach the metal-centered HOMO shown in Figure 7. Consequently, the synchronous cleavage of the $SiCH_2$−H bond (1.535 Å) and formation of the Ir−CH_2Si (2.398 Å) and Ir−H (1.641 Å) bonds take place along with shift of the CO ligand from the equatorial plane to the axial position.

The treatment of a solution of **4**+**5** with CO (1 atm, 12 h) yields the formal elimination of HCl and the quantitative formation of the pentacoordinated iridium(I) dicarbonyl complex **6** still featuring the metalated [SiNP−H] ligand (Scheme 4).[13] The solid-state structure of **6** has been

dx.doi.org/10.1021/ic4024458 | Inorg. Chem. 2014, 53, 972−980

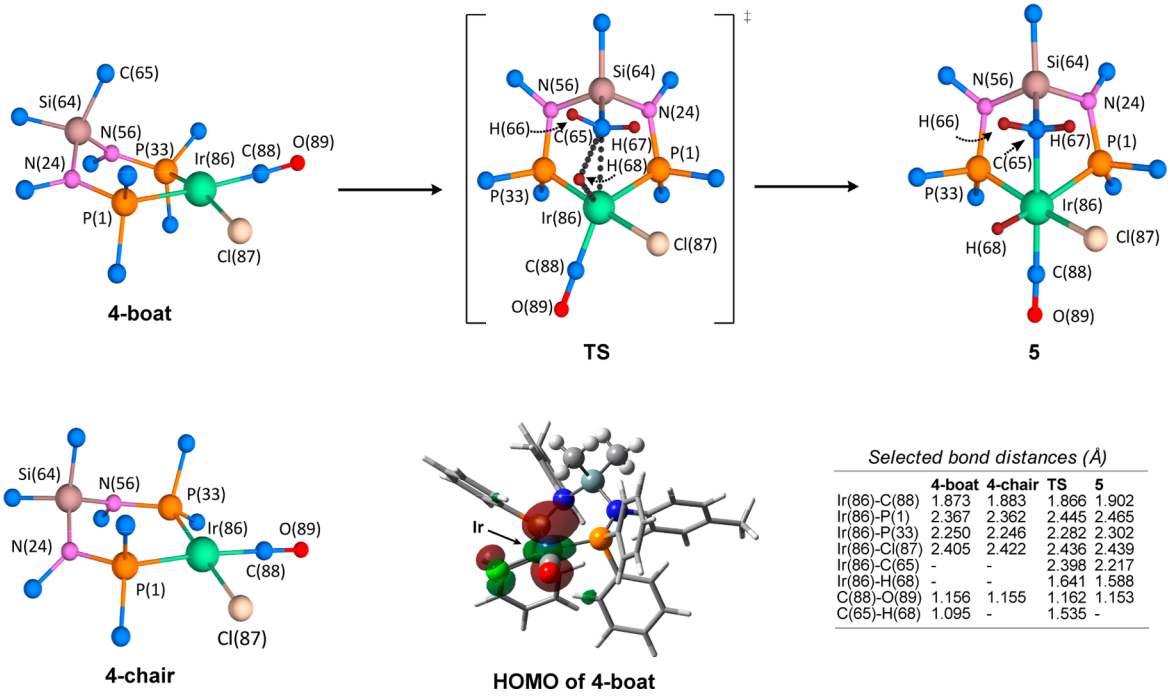

Selected bond distances (Å)

	4-boat	4-chair	TS	5
Ir(86)-C(88)	1.873	1.883	1.866	1.902
Ir(86)-P(1)	2.367	2.362	2.445	2.465
Ir(86)-P(33)	2.250	2.246	2.282	2.302
Ir(86)-Cl(87)	2.405	2.422	2.436	2.439
Ir(86)-C(65)	-	-	2.398	2.217
Ir(86)-H(68)	-	-	1.641	1.588
C(88)-O(89)	1.156	1.155	1.162	1.153
C(65)-H(68)	1.095	-	1.535	-

Figure 7. Optimized structures of IrCl(CO)(SiNP) (**4**), IrHCl(CO)(SiNP−H) (**5**), and the transition state for the transformation **4** ⇆ **5** along with the calculated HOMO of the boat conformer of **4**. Selected bond distances (Å) are given in the table, and selected angles (deg) are in order: C(65)−Ir(86)−C(88), 175.1 (**5**), 152.0 (**TS**); C(65)−Ir(86)−Cl(87), 89.5 (**5**), 92.2 (**TS**). Hydrogen atoms are omitted, and only *ipso* carbon atoms of the aromatic rings are shown for clarity (for atomic coordinates, see the Supporting Information).

determined by single-crystal X-ray diffraction, and its molecular structure is shown in Figure 8. Table 1 contains selected bond distances and angles.

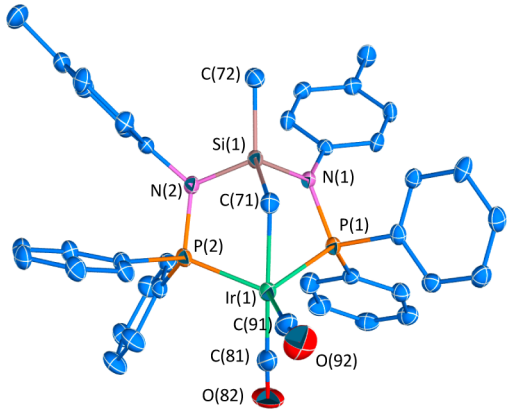

Figure 8. ORTEP views of Ir(SiNP−H)$(CO)_2$ (**6**) with the numbering scheme adopted and the thermal ellipsoids at 50% probability.

The [SiNP−H] ligand features a tridentate κ^3C,P,P' coordination mode involving both the two phosphorus atoms and the carbon atom of the $SiCH_2$ moiety. Interestingly, the P(1), P(2), and C(71) atoms show a distorted *fac* arrangement at the metal center with an expanded P(1)−Ir(1)−P(2) angle (106.61°) and compressed P(1)−Ir(1)−C(71) and P(2)−Ir(1)−C(71) angles (79.45°, 82.65°) with respect to the ideal 90° value, reasonably due to the presence of two fused five-membered rings, Ir(1)−P(1)−N(1)−Si(1)−C(71) and Ir(1)−P(2)−N(2)−Si(1)−C(71). The coordination sphere at the metal center is completed by two CO ligands, one occupying

Table 1. Selected Bond Angles (deg) and Distances (Å) of Ir(SiNP−H)$(CO)_2$ (6)

Ir(1)−C(81) 1.885(5)	N(1)−C(51) 1.418(4)
Ir(1)−C(91) 1.885(5)	N(2)−C(61) 1.441(4)
Ir(1)−C(71) 2.185(4)	C(81)−O(82) 1.135(5)
Ir(1)−P(1) 2.290(2)	C(91)−O(92) 1.145(5)
Ir(1)−P(2) 2.3100(19)	C(71)−Si(1)−C(72) 120.59(17)
P(1)−N(1) 1.691(3)	C(81)−Ir(1)−C(91) 100.09(19)
P(1)−C(11) 1.811(4)	C(81)−Ir(1)−C(71) 173.53(16)
P(1)−C(21) 1.815(4)	C(91)−Ir(1)−C(71) 85.91(16)
P(2)−N(2) 1.701(3)	C(81)−Ir(1)−P(1) 95.34(13)
P(2)−C(41) 1.809(4)	C(91)−Ir(1)−P(1) 120.10(13)
P(2)−C(31) 1.823(4)	C(71)−Ir(1)−P(1) 79.45(11)
Si(1)−N(2) 1.756(3)	C(81)−Ir(1)−P(2) 95.29(13)
Si(1)−N(1) 1.766(3)	C(91)−Ir(1)−P(2) 128.67(14)
Si(1)−C(71) 1.830(4)	C(71)−Ir(1)−P(2) 82.65(10)
Si(1)−C(72) 1.842(4)	P(1)−Ir(1)−P(2) 106.61(7)

the position trans to C(71) and the other in the equatorial plane of the molecule, the overall coordination polyhedron being a distorted trigonal bypiramid (TBPY-5-23). With this respect, it is worth mentioning that Ir(1) lays approximately 0.3 Å out of the equatorial plane, slightly shifted toward the C(81) atom. As far as bond distances are concerned, related structurally characterized iridium(I) complexes, such as Ir{$C_6H_3(CH_2P(CF_3)_2)_2$}$(CO)_2$[14] and Ir(CF_2CF_2H)-$(CO)_2(PPh_3)_2$,[15] feature similar Ir−C−O, Ir−P, and Ir−C bond distances, although with different coordination polyhedra or ligands' distribution around the metal center. On the other hand, the Si(1)−C(71) and Si(1)−C(72) are very similar to the silicon−carbon bond distances observed in $RhCl_2(\eta^3-C_3H_5)$(SiNP) (1.854; 1.839 Å).[3] Nevertheless, a severe distortion of the C−Si−C angle is observed. Indeed, the C−

dx.doi.org/10.1021/ic4024458 | *Inorg. Chem.* 2014, 53, 972−980

Si−C angle in $RhCl_2(\eta^3\text{-}C_3H_5)$(SiNP) is 108.02°, whereas the C(71)−Si(1)−C(72) angle in Ir(SiNP−H)$(CO)_2$ is 120.59°, thus suggesting that the coordination of the methylene moiety to iridium entails a significant expansion of the C−Si−C angle. For the sake of comparison, it should be mentioned that when comparing angles and bond distances of the $[IrP_2(CH_2)(CO^{ax})]$ moiety in the calculated structure of **5** with those in the solid-state structure of **6**, very small differences (≤3%) were observed, major deviations being observed only for one of the two Ir−P bond distances (that for the phosphorus trans to the hydride ligand in **5**) and the P−Ir−P angle (wider in **6** due to the less congested coordination sphere at the metal center).

Finally, the solid-state structure of **6** is maintained in solution. Indeed, two IR absorptions (CH_2Cl_2) were observed at 1927 and 2001 cm^{-1} (ν_{CO}) in agreement with the presence of a $Ir(CO)_2$ moiety in an environment of C_s symmetry. Further, the ^1H, $^{13}C\{^1H\}$, and $^{31}P\{^1H\}$ NMR spectra indicate a *fac* symmetrically coordinated [SiNP−H] ligand; that is, both the two N−P arms of the ligand and the protons of the $IrCH_2$ moiety are equivalent (see Experimental Section).[4]

In relation to the C−H activation in the coordinated SiNP ligand, it is worth mentioning that, to the best of our knowledge, the intramolecular C−H addition of a methyl moiety from a coordinated diphosphane ligand to a group 9 metal has previously been reported only in rhodium complexes containing the ligands 1,3-$(CH_2P^tBu_2)_2(C_6H_4)$ or 1,3-$(CH_2P^tBu_2)$-4,6-$(CH_3)_2(C_6H_2)$.[16] The ability of both diphosphano ligands to adopt a trans-spanning coordination mode and their rigidity were found to be decisive in getting the CH_3 moiety close to the metal center, and finally in promoting the addition of the C−H bond to the metal center (Scheme 5).[16]

Scheme 5

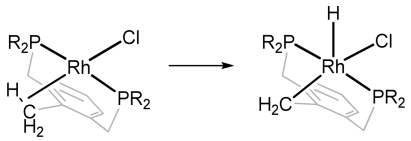

On the contrary, SiNP tends to coordinate the metal center occupying two cis sites, and the boat conformation of the SiN_2P_2Ir is the necessary requisite to allow the $SiCH_2$−H group to approach the metal center and finally add to the metal center.

CONCLUSIONS

The *N*,*N*′-diphosphanosilanediamine ligand $SiMe_2\{N(4\text{-}C_6H_4CH_3)PPh_2\}_2$ (SiNP) is able to coordinate iridium(I) affording tetra- or pentacoordinated complexes (**1**$^+$, **2**, and **3**$^+$). The solution structure of the pentacoordinated complexes of formula $[IrX(SiNP)(cod)]^{n+}$ (**2**, X = Cl, *n* = 0; **3**$^+$, X = CO, *n* = 1) depends on the nature of the ancillary ligand X. Indeed, the chlorido ligand occupies the apical position of a square planar pyramid, while the trigonal bypiramydal structure is the favored one with the CO ligand, in both cases a boat conformation being adopted by the SiN_2P_2Ir ring. Different fluxional processes for **2** and **3**$^+$ are observed in solution as a consequence of the different geometries at the metal center: indeed, the reversible dissociation of one phosphorus atom of the SiNP ligand in IrCl(cod)(SiNP) (**2**) was calculated to be the process averaging the up and down semispaces both at the cod and at the SiNP ligands. On the other hand, the interconversion(s) between pentacoordinated isomers should be responsible for the averaged ^1H and ^{31}P NMR spectra of **3**$^+$ at room temperature.

Starting from the carbonyl species $[Ir(CO)(cod)(SiNP)]^+$ (**3**$^+$), the C−H addition to the iridium(I) center easily takes place at room temperature when the chloride ion is present in solution, either as the counter-ion in [**3**]Cl or if added as [PPN]Cl to [**3**][PF_6]. Under these conditions, the preliminary formation of the tetracoordinated carbonyl complex IrCl(CO)(SiNP) (**4**) has been observed along with the consequent formation of the hydride complex IrHCl(CO)(SiNP−H) (**5**) via the synchronous cleavage of the $SiCH_2$−H bond, the formation of the Ir−CH_2Si and Ir−H bonds, and the shift of the CO ligand from the equatorial plane in **4** to the axial coordination site in **5**.

Finally, the κ^3C,P,P' coordination mode of the [SiNP−H] ligand has been fully characterized in the solid state in the pentacoordinated dicarbonyl iridium(I) complex Ir(SiNP−H)$(CO)_2$ (**6**) showing that it easily fits three mutually cis coordination sites and that a severe distortion of the C−Si−C angle is necessary to accommodate the methylene moiety in the coordination sphere of the metal center.

The influence of the ancillary ligands on the C−H bond activation and the application of the resulting Ir[κ^3C,P,P'-(SiNP−H)] platform to both stoichiometic and catalytic processes is being investigated, and results will be published in due course.

EXPERIMENTAL SECTION

All of the operations were carried out using standard Schlenk-tube techniques under an atmosphere of prepurified argon or in a Braun glovebox under dinitrogen or argon. The solvents were dried and purified according to standard procedures. [PPN]Cl (Aldrich) and CO (Praxair) were commercially available and were used as received. The compounds $[IrCl(cod)]_2$,[17] $[Ir(cod)(CH_3CN)_2][PF_6]$,[18] and SiNP[3] were prepared as previously described in the literature. NMR spectra were measured with Bruker spectrometers (AV300, AV400, AV500) and are referred to as $SiMe_4$ (^1H, ^{13}C), H_3PO_4 (^{31}P), and $CFCl_3$ (^{19}F). ^1H and ^{13}C data are given together in the following way: δ_H (multiplicity, ^1H-assignment, number of hydrogen, δ_C). Only the quaternary carbon atoms (when observed) are given in the $^{13}C\{^1H\}$ NMR subsection. The diffusion experiments were performed using the stimulated echo pulse sequence[19] without spinning, and the collected data were treated as previously described.[3] The hydrodynamic radius (R_h) was calculated using the equation of Stokes−Einstein, and the radius of gyration (R_g) was calculated according the literature, using optimized molecular structures.[20] Infrared spectra were recorded on a ThermoNicolet Avatar 360 FT-IR spectrometer. Elemental analyses were performed by using a Perkin-Elmer 2400 microanalyzer.

Synthesis of [Ir(cod)(SiNP)][PF_6] ([1][PF_6]). A solution of SiNP (150 mg, 0.235 mmol, 638.79 g/mol) in CH_2Cl_2 (10 mL) was added to $[Ir(cod)(CH_3CN)_2][PF_6]$ (124 mg, 0.235 mmol, 527.47 g/mol). After 30 min of stirring, the resulting deep orange solution was evaporated, and the resulting solid was washed with hexane (3 × 5 mL). The deep orange solid was dried under a vacuum and identified as $[Ir(cod)(SiNP)][PF_6]$ ([**1**][PF_6], 224 mg, 88% yield). Anal. Calcd for $C_{48}H_{52}F_6IrN_2P_3Si$ (1084.15): C, 53.18; H, 4.83; N, 2.58. Found: C, 53.02; H, 5.00; N, 2.52. ^1H NMR (CD_2Cl_2, 298 K): δ7.30−7.51 (20H, PPh, δ_C = 128.2, *m*-PPh, 131.5, *p*-PPh, 133.7, *o*-PPh), 6.85 (d, 8.2 Hz, 4H, C^3H^{tol}, δ_C = 129.4), 6.68 (d, 8.2 Hz, 4H, C^2H^{tol}, δ_C = 129.6), 4.31 (br, 4H, $C^{sp2}H^{cod}$, δ_C = 88.6), 2.28−2.15 (10H, $C^{sp3}H^{cod}$ + CH_3^{tol}, δ_C = 20.4, CH_3^{tol}), 2.07 (m, 4H, $C^{sp3}H^{cod}$, δ_C = 30.8), −0.67 (s, 6H, $SiCH_3$, δ_C = 3.7). ^{19}F NMR (CD_2Cl_2, 298 K): δ −73.5 (d, 710.5 Hz). $^{31}P\{^1H\}$ NMR (CD_2Cl_2, 298 K): δ 53.5 (s, SiNP), −144.4 (sp, 710.5 Hz, PF_6^-). *D* ($CDCl_3$, 298 K) = (5.94 ± 0.03) × 10^{-6} cm^2 s^{-1}, R_h = 6.45 ± 0.03 Å (R_g = 6.33 Å).

dx.doi.org/10.1021/ic4024458 | *Inorg. Chem.* 2014, 53, 972−980

Synthesis of IrCl(cod)(SiNP)(2). A suspension of SiNP (466 mg, 0.730 mmol, 638.79 g/mol) in CH_2Cl_2 (5 mL) was added to $[IrCl(cod)]_2$ (252 mg, 0.375 mmol, 671.70 g/mol). The mixture was stirred for 1 h, and the resulting solid was filtered off, dried in vacuo, and identified as IrCl(cod)(SiNP) (**2**, 498 mg, 70% yield). Anal. Calcd for $C_{48}H_{52}ClIrN_2P_2Si$ (974.64): C, 59.15; H, 5.38; N, 2.87. Found: C, 59.24; H, 5.33; N, 2.55. ^{1}H NMR ($CDCl_3$, 298 K): δ7.62 (m, 8H, *o*-PPh, δ_C = 134.31), 7.31 (t, $^3J_{HH}$ = 7.1 Hz, 4H, *p*-PPh, δ_C = 129.84), 7.22 (t, $^3J_{HH}$ = 7.1 Hz, 8H, *m*-PPh, δ_C = 126.99), 6.69 (d, 7.4 Hz, 4H, C^3H^{tol}, δ_C = 128.69), 6.57 (d, 7.4 Hz, 4H, C^2H^{tol}, δ_C = 130.9), 3.42 (br, 4H, $C^{sp2}H^{cod}$, δ_C = 74.97), 2.25−2.06 (10H, CH_3^{tol} + $C^{sp3}H_2^{cod}$, δ_C = 20.74, CH_3^{tol}, 31.58, $C^{sp3}H_2^{cod}$), 1.74 (m, 4H, $C^{sp3}H_2^{cod}$), 0.39 (s, 6H, $SiCH_3$, δ_C = 4.21). ^{31}P NMR ($CDCl_3$, 298 K): δ49.4 (s). *D* (CD_2Cl_2, 298 K) = (8.87 ± 0.21) × 10^{-6} cm^2 s^{-1}, R_h = 5.72 ± 0.14 Å (R_g = 5.97 Å).

Synthesis of [Ir(CO)(cod)(SiNP)][PF_6] ([3][PF_6]). A solution of [Ir(cod)(SiNP)][PF_6] (156 mg, 0.144 mmol, 1084.15 g/mol) in CH_2Cl_2 (3 mL) was stirred under an atmosphere of CO (1 atm) for 20 min. A pale yellow solution was obtained, which was partially evaporated and added to hexane (10 mL) affording a yellow solid identified as [Ir(CO)(cod)(SiNP)][PF_6] ([**3**][PF_6], 147 mg, 92% yield). Anal. Calcd for $C_{49}H_{52}F_6IrN_2OP_3Si$ (1112.16): C, 52.92; H, 4.71; N, 2.52. Found: C, 53.01; H, 4.92; N, 2.48. ν_{CO} (CH_2Cl_2), 1994 cm^{-1}. ^{1}H NMR (CD_2Cl_2, 298 K): δ 7.36−7.69 (PPh, 20H, δ_C = 134.98, *m*-PPh; 132.48, *m*-PPh; 128.31, *o*-PPh; 128.11, *o*-PPh; 132.12, *p*-PPh; 131.57 or 131.64, *p*-PPh), 6.97 (d, 8.2 Hz, 2H, C^3H^{tol}, δ_C = 129.54), 6.92 (d, 8.2 Hz, 2H, C^2H^{tol}, δ_C = 131.57 or 131.64), 6.77 (d, 8.2 Hz, 2H, C^3H^{tol}, δ_C = 129.34), 6.18 (d, 8.2 Hz, 2H, C^2H^{tol}, δ_C = 131.33), 3.86 (br, 4H, $C^{sp2}H^{cod}$, δ_C = 82.90), 2.22 (s, CH_3^{tol}, 6H, δ_C = 20.52), 2.05 (m, 4H, $C^{sp3}H^{cod}$, δ_C = 32.51), 1.93 (m, $C^{sp3}H^{cod}$, 4H, δ_C = 32.51), 0.56 (s, 3H, $SiCH_3$, δ_C = 1.24), −0.29 (s, 3H, $SiCH_3$, δ_C = 3.26). ^{13}C{^{1}H} NMR (CD_2Cl_2, 298 K): δ 179.4 (t, 4.6 Hz, CO). ^{31}P{^{1}H} NMR (CD_2Cl_2, 298 K): δ 39.4 (s, SiNP), −144.4 (sp, 710.5 Hz, PF_6^-). *D* (CD_2Cl_2, 298 K) = (7.89 ± 0.06) × 10^{-6} cm^2 s^{-1}, R_h = 6.43 ± 0.04 Å (R_g = 6.31 Å). Selected ^{1}H NMR data at 183 K (CH_2Cl_2): δ 4.25 (br, 1H, $C^{sp2}H^{cod}$), 3.11 (br, 1H, $C^{sp2}H^{cod}$), 2.22 (s, 3H, CH_3^{tol}), 2.01 (s, 3H, CH_3^{tol}), 1.82 (br, 1H, $C^{sp2}H^{cod}$), 1.35 (br, 1H, $C^{sp2}H^{cod}$), 0.20 (s, 3H, $SiCH_3$), −0.35 (s, 3H, $SiCH_3$).

Reaction of IrCl(cod)(SiNP) with CO. *a. Synthesis of [Ir(CO)(cod)(SiNP)]Cl ([**3**]Cl).* A suspension of IrCl(cod)(SiNP) (159 mg, 0.163 mmol, 974.64 g/mol) in CH_2Cl_2 (5 mL) was degassed and contacted with CO (1 atm). As soon as the dissolution of the solid was observed (approx. 30 min), all volatiles were removed in vacuo, and the resulting solid was washed with hexane (3 × 5 mL), dried in vacuo, and finally identified as [Ir(CO)(cod)(SiNP)]Cl ([**3**]Cl, 151 mg, 92% yield). Anal. Calcd for $C_{49}H_{52}ClIrN_2OP_2Si$ (1002.65): C, 58.70; H, 5.23; N, 2.79. Found: C, 59.00; H, 5.11; N, 2.68. ν_{CO} (CH_2Cl_2), 1994 cm^{-1}. ^{1}H and ^{31}P NMR spectra of a freshly prepared solution of [**3**]Cl in CD_2Cl_2 are very similar to those measured for [**3**][PF_6].

*b. Formation of [IrCl(CO)(SiNP)] (**4**) and IrHCl(CO)(SiNP−H) (**5**).* A suspension of IrCl(cod)(SiNP) (**2**, 220 mg, 0.226 mmol, 974.64 g/mol) in CH_2Cl_2 (5 mL) was degassed and contacted with CO (1 atm). As soon as the dissolution of the solid was observed (approx. 30 min), CO gas was replaced by argon gas, and the solution was stirred for about 12 h. Finally, all volatiles were removed in vacuo, and the resulting solid was washed with hexane (3 × 5 mL), dried in vacuo, and finally identified as a mixture of [IrCl(CO)(SiNP)] (**4**, 80%) and IrHCl(CO)(SiNP−H) (**5**, 20%) (157 mg, 78% yield). Anal. Calcd for $C_{41}H_{40}ClIrN_2OP_2Si$ (894.47): C, 55.05; H, 4.51; N, 3.13. Found: C, 55.15; H, 4.68; N, 3.15.

IrCl(CO)(SiNP) (4). ν_{CO} (CH_2Cl_2), 2007 cm^{-1}. ^{31}P{^{1}H} NMR (CD_2Cl_2, 298 K): δ 63.4 (d, $^2J_{PP}$ = 30.5, P^1), 41.2 (d, $^2J_{PP}$ = 30.5, P^2). *D* (CD_2Cl_2, 298 K) = (8.58 ± 0.03) × 10^{-6} cm^2 s^{-1}, R_h = 5.91 ± 0.02 Å (R_g = 5.92 Å). Selected NMR data (δ_H, bold type, and δ_C, italics type) are shown in the following scheme.

IrHCl(CO)(SiNP−H) (5). ν_{CO} (CH_2Cl_2), 2026 cm^{-1}. ^{31}P{^{1}H} NMR (CD_2Cl_2, 298 K): δ 48.1 (d, $^2J_{PP}$ = 9.0, P^1), 43.0 (d, $^2J_{PP}$ = 9.0, P^2). *D* (CD_2Cl_2, 298 K) = (8.45 ± 0.11) × 10^{-6} cm^2 s^{-1}, R_h = 6.00 ± 0.08 Å (R_g = 6.04 Å). Selected NMR data (δ_H, bold type, and δ_C, italics type) are shown in the following scheme.

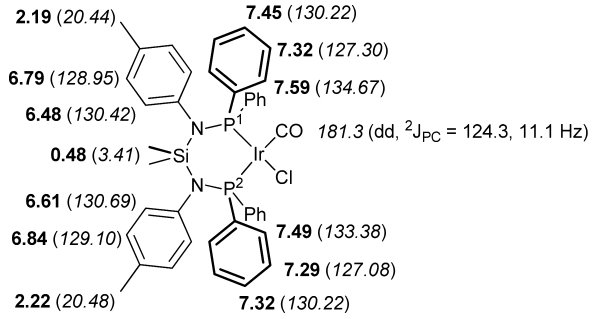

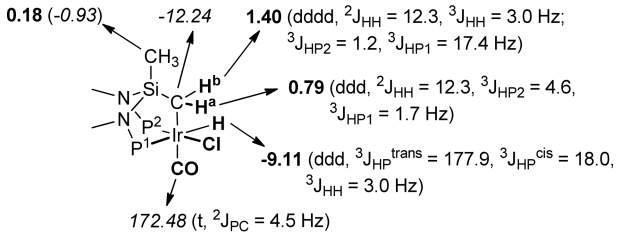

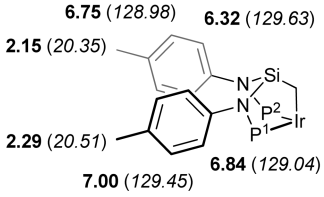

*c. Synthesis of Ir(SiNP−H)(CO)$_2$ (**6**).* A suspension of IrCl(cod)(SiNP) (185 mg, 0.190 mmol, 974.64 g/mol) in CH_2Cl_2 (5 mL) was degassed, contacted with CO (1 atm), and stirred at room temperature for 18 h affording a deep yellow solution. The solution was partially evaporated (approx. 2 mL left) and layered with hexane. After 2 days, bright yellow crystals precipitated out. The supernatant solution was decanted, and the crystals were washed with hexane, dried in vacuo, and identified as Ir(SiNP−H)$(CO)_2$ (**6**, 138 mg, 82% yield). Anal. Calcd for $C_{42}H_{39}IrN_2O_2P_2Si$ (886.02): C, 56.93; H, 4.44; N, 3.16. Found: C, 56.02; H, 4.45; N, 3.28. ν_{CO} (CH_2Cl_2), 2001, 1927 cm^{-1}. ^{1}H NMR ($CDCl_3$, 298 K): δ 7.57 (m, 4H, *o*-PPh^{endo}, δ_C = 133.87), 7.42−7.29 (10H, *o*-PPh^{exo} + *m*-PPh^{endo} + *p*-PPh^{exo}, δ_C = 131.97, *o*-PPh, 127.56, *m*-PPh, 129.83, *p*-PPh), 7.15 (m, 4H, *m*-PPh^{exo}, δ_C = 127.41), 7.25 (m, 2H, *p*-PPh^{endo}, δ_C = 129.83), 6.84 (d, 4H, $^3J_{HH}$ = 8.1 Hz, C^3H^{tol}, δ_C = 128.86), 6.55 (d, 4H, $^3J_{HH}$ = 8.1 Hz, C^2H^{tol}, δ_C = 129.37), 2.21 (s, 6H, CH_3^{tol}, δ_C = 20.76), 0.61 (t, 2H, $^3J_{HP}$ = 10.2 Hz, $SiCH_2Ir$, δ_C = 0.14, t, $^2J_{CP}$ = 8.1 Hz), −0.36 (s, 3H, $SiCH_3$, δ_C = 26.7). ^{31}P{^{1}H} NMR ($CDCl_3$, 298 K): δ 49.6 (s).

X-ray Measurements and Structure Determination of Ir(SiNP−H)$(CO)_2$ (6). Single crystals of Ir(SiNP−H)$(CO)_2$ (**6**) were obtained by layering hexane over a CH_2Cl_2 solution of **6**. Intensities were collected at 100 K using a Bruker SMART APEX diffractometer with graphite-monochromated Mo Kα radiation (λ = 0.71073 Å) following standard procedures. Intensities were integrated and corrected for absorption effects using the SAINT+[21] and SADABS[22] programs, included in the APEX2 package. The structure was solved by standard direct methods. All non-H atoms were located in the subsequent Fourier maps. Refinement was carried out by full-matrix least-square procedure (based on F_0^2) using anisotropic temperature factors for all non-hydrogen atoms. The H atoms were placed in calculated positions with fixed isotropic thermal parameters ($1.2U_{equiv}$) of the parent carbon atom. Calculations were performed with the SHELX-97[23] program implemented in the WinGX[24] package.

Crystal Data for 6. $C_{42}H_{39}IrN_2O_2P_2Si$, M = 885.98 g mol^{-1}; pale yellow needle, 0.15 × 0.17 × 0.40 mm^3; triclinic, $P\bar{1}$; a = 12.007(12) Å, b = 12.770(12) Å, c = 12.878(12) Å, α = 102.208(11)°, β = 100.476(11)°, γ = 100.405(11)°; Z = 2; V = 1848(3) $Å^3$; D_c = 1.592 g cm^{-3}; μ = 3.771 mm^{-1}, minimum and maximum absorption correction

dx.doi.org/10.1021/ic4024458 | Inorg. Chem. 2014, 53, 972−980

factors 0.416 and 0.568; $2\theta_{max}$ = 57.22°; 21 576 collected reflections, 8627 unique (R_{int} = 0.0358); 8627/0/454 data/restraints/parameters; final GOF = 1.059; R1 = 0.0318 (7665 reflections, $I > 2\sigma(I)$); wR2 = 0.0754 for all data. CCDC refcode 941530.

DFT Geometry Optimization. The molecular structures were optimized at the ONIOM(BP3LYP/GenECP:UFF) level using the Gaussian 09 program.[25] The aromatic rings were included in the low level layer and the remaining atoms in the high level layer. The LanL2TZ(f) basis and pseudo potential were used for iridium and the 6-31G(d,p) basis set for the remaining atoms. Stationary points were characterized by vibrational analysis (transition states featuring one imaginary frequency, minimum energy molecular structures featuring only positive frequencies).

■ ASSOCIATED CONTENT

Supporting Information

Selected NMR and kinetic data, the CIF file for the structure of **6**, and atomic coordinates of the optimized structures. This material is available free of charge via the Internet at http://pubs.acs.org.

■ AUTHOR INFORMATION

Corresponding Author

*Tel.: +34 976 739863. E-mail: passarel@unizar.es.

Notes

The authors declare no competing financial interest.

■ ACKNOWLEDGMENTS

Financial support from the Spanish "Ministerio de Economía y Competitividad" (CTQ2010-15221) and "Diputación General de Aragón" (Group E07) is gratefully acknowledged. V.P. is indebted to Dr. Pablo Sanz (ISQCH, Universidad de Zaragoza) for insightful comments and useful discussions about the X-ray determination of complex **6**.

■ REFERENCES

(1) (a) Carter, E.; Cavell, K.; Gabrielli, W. F.; Hanton, M. J.; Hallett, A. J.; McDyre, L.; Platts, J. A.; Smith, D. M.; Murphy, D. M. *Organometallics* **2013**, *32*, 1924−1931. (b) Cloete, N.; Visser, H. G.; Engelbrecht, I.; Overett, M. J.; Gabrielli, W. F.; Roodt, A. *Inorg. Chem.* **2013**, *52*, 2268−2270. (c) Mayer, T.; Boettcher, H.-C. *Polyhedron* **2013**, *50*, 507−511. (d) Ogawa, T.; Kajita, Y.; Wasada-Tsutsui, Y.; Wasada, H.; Masuda, H. *Inorg. Chem.* **2013**, *52*, 182−195. (e) Pernik, I.; Hooper, J. F.; Chaplin, A. B.; Weller, A. S.; Willis, M. C. *ACS Catal.* **2012**, *2*, 2779−2786. (f) Todisco, S.; Gallo, V.; Mastrorilli, P.; Latronico, M.; Re, N.; Creati, F.; Braunstein, P. *Inorg. Chem.* **2012**, *51*, 11549−11561. (g) Do, L. H.; Labinger, J. A.; Bercaw, J. E. *Organometallics* **2012**, *31*, 5143−5149. (h) Trentin, F.; Chapman, A. M.; Scarso, A.; Sgarbossa, P.; Michelin, R. A.; Strukul, G.; Wass, D. F. *Adv. Synth. Catal.* **2012**, *354*, 1095−1104. (i) Bowen, L. E.; Charernsuk, M.; Hey, T. W.; McMullin, C. L.; Orpen, A. G.; Wass, D. F. *Dalton Trans.* **2012**, *39*, 560−567. (j) Aluri, B.; Peulecke, N.; Muller, B. H.; Peitz, S.; Spannenberg, A.; Hapke, M.; Rosenthal, U. *Organometallics* **2012**, *29*, 226−231. (k) Cheung, H. W.; So, C. M.; Pun, K. H.; Zhou, Z.; Lau, C. P. *Adv. Synth. Catal.* **2011**, *353*, 411−425. (l) Gopalakrishnan, J. *Appl. Organomet. Chem.* **2009**, *23*, 291−318. (m) Ozerov, O. V.; Guo, C.; Foxman, B. M. *J. Organomet. Chem.* **2006**, *691*, 4802−4806. (n) Bollmann, A.; Blann, K.; Dixon, J. T.; Hess, F. M.; Killian, E.; Maumel, H.; McGuiness, D. S.; Morgan, D. H.; Neveling, A.; Otto, S.; Overett, M.; Slawin, A. M. Z.; Wasserscheid, P.; Kuhlmann, S. *J. Am. Chem. Soc.* **2004**, *126*, 14712−14713. (o) Slawin, A. M. Z.; Wainwright, M.; Woolins, J. D. *J. Chem. Soc., Dalton Trans.* **2002**, 513−51.

(2) (a) Aucott, S. M.; Clarke, M. L.; Slawin, A. M. Z.; Woolins, J. D. *J. Chem. Soc., Dalton Trans.* **2001**, 972−976. (b) Clarke, M. L.; Slawin, A. M. Z.; Woolins, J. D. *Phosphorus, Sulfur Silicon Relat. Elem.* **2001**, *168*−*169*, 329−332.

(3) Passarelli, V.; Benetollo, F. *Inorg. Chem.* **2011**, *50*, 9958−9967.

(4) The proposed mononuclear structure agrees with the measured diffusion coefficient and with the calculated hydrodynamic radius (see Experimental Section).

(5) Nomenclature of Inorganic Chemistry. *IUPAC Recommendations 2005*; Connely, N. G., Damhus, T., Eds.; Royal Society of Chemistry: Cambridge, 2005.

(6) Makino, T.; Yamamoto, Y.; Itoh, K. *Organometallics* **2004**, *23*, 1730−1737.

(7) Shibata, T.; Yamashita, K.; Ishida, H.; Takagi, K. *Org. Lett.* **2001**, *3*, 1217−1219.

(8) As observed for $[Ir(cod)(SiNP)]^+$ (**1**), the boat conformation of the SiN_2P_2Ir ring in the SPY-5-13 optimized structure of IrCl(cod)(SiNP) (**2**) is more stable than the chair conformation (+38 kJ mol^{-1}).

(9) The calculated ν_{CO} wavenumber for the TBPY-5-12 structure is 1998 cm^{-1}, and the experimental value for $\mathbf{3}^+$ is 1994 cm^{-1}.

(10) A similar behavior of [**3**]Cl was observed in THF at room temperature.

(11) Minch, M. J. *Concepts Magn. Reson.* **1994**, *6*, 41−56.

(12) The transition state for the reaction IrCl(CO)(SiNP) (**4**) ⇆ IrHCl(CO)(SiNP−H) (**5**) was located at 98.8 kJ mol^{-1} higher than **4**.

(13) It is noteworthy that while [**3**]Cl readily reacts with excess of CO affording **6** after 12 h of exposure to a CO atmosphere, [**3**][PF_6] do not react with CO even after prolonged exposure to a CO atmosphere, thus indicating that the presence of the chloride ion is essential to obtain **6**.

(14) CCDC refcode ATOQUV, in: Adams, J. J.; Arulsamy, N.; Roddick, D. M. *Organometallics* **2011**, *30*, 697−711.

(15) CCDC refcode JEPTIH, in: Burrell, A. K.; Roper, W. R. *Organometallics* **1990**, *9*, 1905−1910.

(16) (a) Sundermann, A.; Uzan, O.; Milstein, D.; Martin, J. M. L *J. Am. Chem. Soc.* **2000**, *122*, 7095−7104. (b) Rybtchinski, B.; Milstein, D. *J. Am. Chem. Soc.* **1999**, *121*, 4528−4529. (c) van der Boom, M. E.; Liou, S.-Y.; Ben−David, Y.; Gozin, M.; Milstein, D. *J. Am. Chem. Soc.* **1998**, *120*, 13415−13421.

(17) Herde, J. L.; Lambert, J. C.; Senoff, C. V. *Inorg. Synth.* **1974**, *15*, 18−20.

(18) Day, V. W.; Klemperer, W. G.; Main, D. J. *Inorg. Chem.* **1990**, *29*, 2345−2355.

(19) (a) Stilbs, P. *Prog. Nucl. Magn. Reson. Spectrosc.* **1987**, *19*, 1−45. (b) Price, W. S. *Concepts Magn. Reson.* **1997**, *9*, 299−336. (c) Price, W. S. *Concepts Magn. Reson.* **1998**, *10*, 197−237. (d) Johnson, C. S., Jr. *Prog. Nucl. Magn. Reson. Spectrosc.* **1999**, *34*, 203−256. (e) Cohen, Y.; Avram, L.; Frish, L. *Angew. Chem.* **2005**, *117*, 524−560. (f) Cohen, Y.; Avram, L.; Frish, L. *Angew. Chem., Int. Ed.* **2005**, *44*, 520−554. (g) Pregosin, P. S.; Kumar, P. G. A.; Fernandez, I. *Chem. Rev.* **2005**, *105*, 2977−2998. (h) Macchioni, A.; Ciancaleoni, G.; Zuccaccia, C.; Zuccaccia, D. *Chem. Soc. Rev.* **2008**, *37*, 479−489.

(20) Ortega, A.; Amoros, D.; García de la Torre, J. *Biophys. J.* **2011**, *101*, 892−898.

(21) *SAINT+, version 6.01*; Bruker AXS, Inc.: Madison, WI, 2001.

(22) Sheldrick, G. M. *SABADS*; University of Göttingen: Göttingen, Germany, 1999.

(23) (a) Sheldrick, G. M. *SHELXL-97*; University of Göttingen: Göttingen, Germany, 1997. (b) Sheldrick, G. M. *Acta Crystallogr.* **2008**, *A64*, 112−122.

(24) Farrugia, L. J. *J. Appl. Crystallogr.* **1999**, *32*, 837−838.

(25) Frisch, M. J.; et al. *Gaussian 09*, revision A.02; Gaussian, Inc.: Wallingford, CT, 2009.